Title
Advances in a fully integrated intravascular OCT-ultrasound system for cardiovascular imaging

ISBN
9780819488565

Authors
Jing, Joe
Li, Jiawen
Li, Xiang
et al.

Publication Date
2012-02-09

DOI
10.1117/12.911635

Advances in a fully integrated intravascular OCT-Ultrasound system for cardiovascular imaging

Joe Jing[1], Jiawen Li[1], Xiang Li[4], Jiechen Yin[1], Jun Zhang[2], Khiet Hoang[3], Pranav Patel[3], Qifa Zhou[4], Zhongping Chen[1, 2]

[1]*University of California, Irvine, Dept. of Biomedical Engineering, Irvine, California 92697*
[2]*Beckman Laser Institute and the Center for Biomedical Imaging, UC Irvine, CA 92612*
[3]*University of California, Irvine, Division of Cardiology, Medical Center, Orange, California 92868*
[4]*University of Southern California, NIH Ultrasonic Transducer Resource Center and Department of Biomedical Engineering, Los Angeles, California 90089*

Abstract

Intracoronary optical coherence tomography (OCT) and intravascular ultrasound (IVUS) are two popular techniques for the detection and determination of atherosclerosis. IVUS allows visualization of plaques while also providing a large penetration depth to determine plaque volume. Intracoronary OCT provides the ability to capture microscopic features associated with high risk plaque. Traditionally to utilize the benefits of both modalities, separate probes and systems had to be used one at a time to image a vessel. We present work required to create a combined OCT IVUS system capable of simultaneous imaging to detect atherosclerotic plaques. A novel integrated probe of size 0.69 mm OD featuring sequential placement of components was created to acquire co-registered images within small coronary vessels. By utilizing commercial graphics processing units (GPUs) real time visualization of acquired data is possible up to a maximum 48 frames per second per channel. In vitro studies on human coronary artery samples as well as in vivo studies in rabbits and pigs show various plaque buildups in both OCT and IVUS images which match histology results, demonstrating the capabilities of the system.

1. Introduction

Atherosclerosis, the thickening of arterial walls due to the accumulation of fatty materials, is the leading cause of death in the United States and is fast becoming the pre-eminent health problem worldwide. In 2007, 33.6% of deaths reported in the US were a result of cardiovascular disease, and an estimated 82.6 million people are living with some form of the disease [1]. Intravascular ultrasound (IVUS) development has made the technique a standard for atherosclerosis diagnosis because of its ability to determine plaque volume within the arterial wall and amount of stenosis in the lumen. Optical coherence tomography (OCT) has recently been increasingly utilized for offering high resolution details of the microscopic features of various plaques and tissue response to stent placement [2-4]. It has been pointed out that OCT and IVUS are complementary in the application of intravascular imaging, and the combination of the two can offer advantages which cannot be achieved by using either modality alone [5]. An integrated OCT IVUS probe offers the attractive combination of both high resolution imaging of plaques and large penetration depths into vessel walls without the need to retract and reinsert multiple probes. In addition, with the improvements available laser sources, data acquisition times can be greatly reduced, allowing for reduced amounts of flushing and increased patient safety. By utilizing commercial graphics processing units (GPU) we achieve large improvements in computational speed allowing for simultaneous real-time images of the two modalities. In this manuscript, we discuss our integrated OCT-IVUS probe as well as improvements made in processing to achieve fully integrated system capable of imaging at up to 48 frames per second per channel. The imaging ability of our system is demonstrated through the imaging of in vitro human coronary artery samples as well as in ongoing in vivo studies in rabbits and pigs.

2. Experiment Setup

The design of the OCT system has been described in detail previously [6-8]. Briefly, light provided from a swept source laser (Santec Corp., 13 mW average power, 100 nm FWHM, 20 kHz) is fed into a 1x2 coupler with 80

Optical Coherence Tomography and Coherence Domain Optical Methods in Biomedicine XVI,
edited by Joseph A. Izatt, James G. Fujimoto, Valery V. Tuchin, Proc. of SPIE Vol. 8213, 82130Y

percent of the light directed towards the sample arm and 20 percent to the reference arm. An adjustable gain photodetector is used for balanced detection of the combined fringe formed from the recirculated light of the sample and reference arms. For the ultrasound system, a Panametrics pulser/receiver is used for the generation of the pulse and subsequent detection of echo signals. The OCT and IVUS signal are fed into separate channels of a 12 bit high speed for simultaneous sampling and the trigger of the laser drives a function generator which serves to synchronize the two systems. A voltage controlled oscillator (VCO) is used to provide an adjustable sample clock for the digitizer in order to fully sample the OCT fringe period.

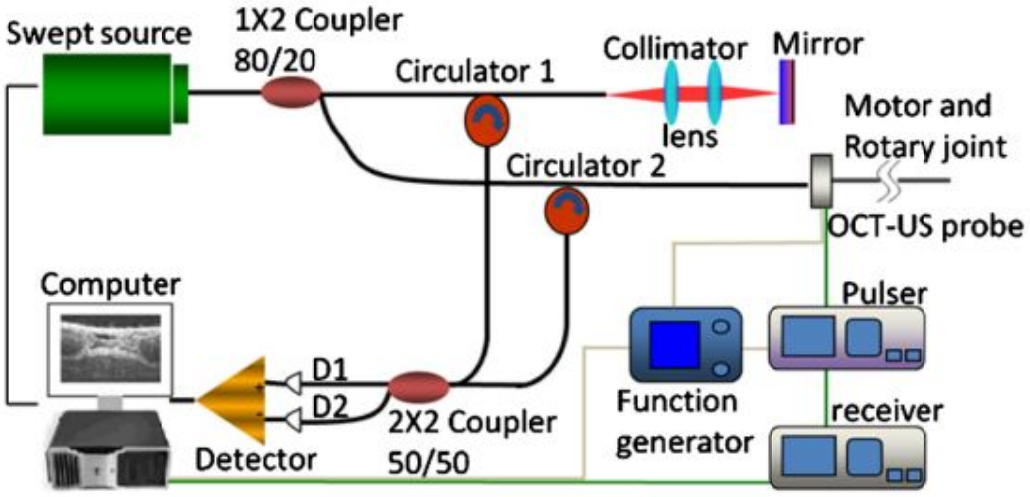

Fig. 1. Combined OCT IVUS system diagram

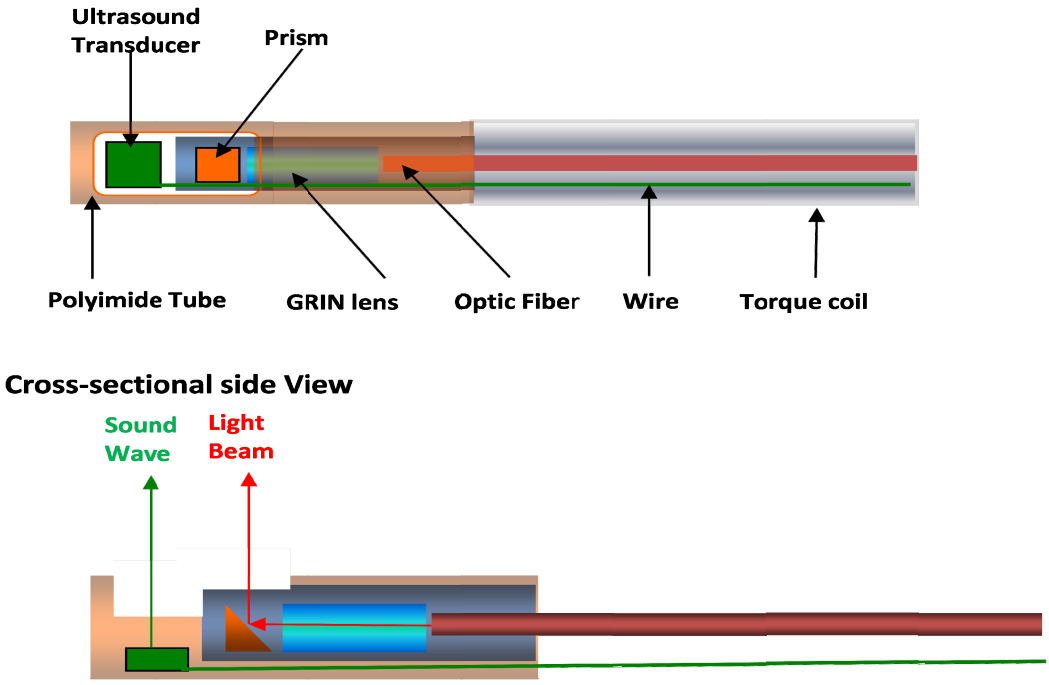

Fig. 2. Integrated OCT IVUS miniaturized probe

The current integrated OCT-IVUS probe features a sequential arrangement allowing for synchronized imaging while also minimizing the overall probe size [8]. The optics for the OCT channel include a 0.35 mm diameter gradient

index lens as well as a 0.3 mm diameter microprism to redirect the light into the tissue and are contained within a 0.41 mm OD polyimide tube. The ultrasound portion of the probe features an ultrasonic transducer built with a PMN-PT single crystal with an aperture of 0.5mm × 0.5mm. The transducer features a 35 MHz center frequency with a fractional bandwidth of 51% and insertion loss of 15 dB. The IVUS transducer was first placed within a 0.69 mm OD polyimide tube followed by OCT portion. A small window was created to allow for both the light beam and sound wave to exit unimpeded. A thin steel tube, 0.61 mm OD, is used for smaller sized tissues to translate torque from the proximal end of the probe to the distal end and to offer protection for both the optical fiber and electrical wires. For studies in larger samples, a 0.69 mm OD double wound flexible torque coil is used to allow for accurate translation of torque to the distal end over a large distance and through tortuous curves. The offset between the IVUS transducer and the OCT prism was measured to be 2 mm to allow for correlating the two images together. The measured sensitivity of the OCT portion is 103 dB with a working distance of 3mm and an axial and lateral resolution of 8 and 30 µm respectively. Resolutions of the US part were 60 and 420 µm, respectively, measured from a 6 µm wire phantom. Rotation of the probe is provided by a DC motor with coupled to a commercial fiber rotary joint through a 2 to 1 gear ratio. Transmission of the electrical pulse and echo signals to and from the IVUS transducer is provided by a brushed electrical slip ring which allows the probe free rotation.

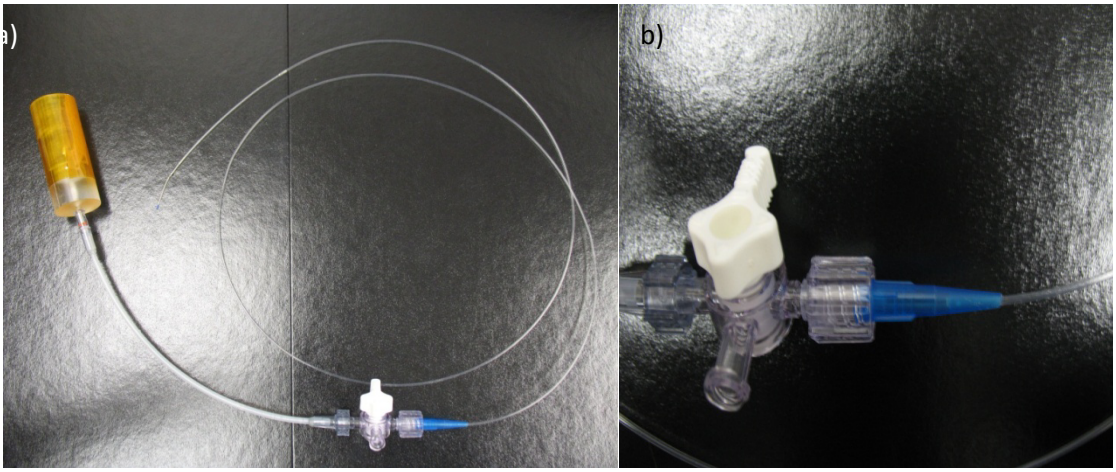

Fig. 3. (a) (b) Added flushing ability incorporated into protective sheath

Additional improvements have been made to the probe design to alleviate some of the challenges experienced during *in vivo* imaging. A flushing mechanism was designed and incorporated with our outer sheath to help remove blood from the imaging area of the probe since OCT image quality and range is highly dependent on the amount scattering blood present. In addition, x-ray markers were also added to the ends of our protective sheaths to allow for guidance into coronary arteries by a commercial C-arm during larger scale models such as pigs. Lastly, a rail was also added into which a standard guide-wire can be inserted for improved positioning and maneuvering of the probe *in vivo*.

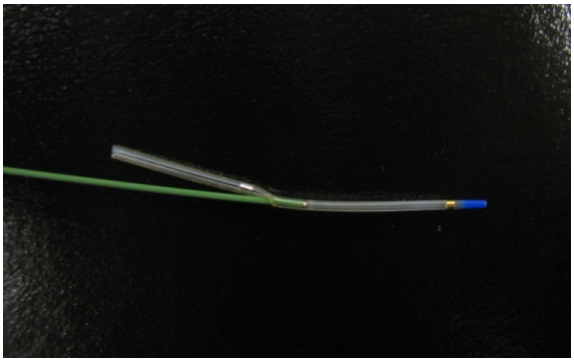

Fig. 4. X-ray detectable marker and guide wire rail

The software that controls the entire system is built from the ground up. The framework and control mechanics are completely written in C++ while the entirety of the data processing is implemented in NVIDIA's CUDA software development kit. Processing of the data occurs on a frame by frame basis, with each frame having 1000 Alines and 8192 points per Aline. The large oversampling factor is necessary for IVUS to image a suitable distance due to the slower propagation of sound waves compared to light. The VCO sampling clock is tuned to provide a 200 MHz clock, which allows for complete sampling of the OCT fringe while also allowing for the data set size to be a power of 2 to speed up Fourier transform calculations. Acquired frames are transferred to the onboard memory of a GPU (NVIDIA GTX 580) for the respective processing. The OCT data first undergoes resampling [9], either by linear interpolation or spline interpolation, to achieve linearity in the K domain followed by the subsequent inverse FFT and logarithmic scaling. The captured IVUS data meanwhile is filtered using a 9^{th} order Butterworth filter with a passband between 20 MHz and 60 MHz to help isolate the echo signal from the pulse followed by a Hilbert transform and logarithmic scaling. Both sets of data are then formatted into bitmaps and transferred back to the host for display. The GPU acts as a massively parallel processor, allowing for very fast arithmetic computations on large data sets. FFT performance on 1000 lines improved from 421 ms on a single thread to 212 µs using the GPU. Logarithm calculations likewise experienced large scaling improvements from 276 ms to 1.05 ms on the GPU.

Both linear and spline OCT resampling were implanted with almost negligible differences due to the large oversampling of the data. Typically spline computation time is much larger than that for linear interpolation. However, by expressing the spline function as the sum of two weighted linear interpolations, we can take advantage of special texture memory built into the GPU [10, 11]. Texture memory is specially designed to improve graphical framerates and provides interpolation in hardware of two adjacent points. By loading a frame into a texture map, the linear interpolation becomes the equivalent of a single memory access which allows spline interpolation to imitate linear interpolation performance, 2.76 ms compared to 2.19 ms respectively for an entire frame. The overall time to process an entire frame from the transfer of data to the GPU until the transfer of the processed bitmaps back into the host's memory is on average 20.94 ms for linear resampling 21.83 ms for spline resampling.

3. Results

Experiments have been conducted in vitro on post-mortem human coronary artery specimens as well as on extracted rabbit samples. In vivo studies have been successfully conducted and repeated on rabbits that have undergone surgery to induce atherosclerotic plaques. Recently, we performed our first in vivo pig study, entering from the femoral artery and working back towards the heart in order to ultimately simulate a possible operation on a human. Removal of blood from the imaging field was accomplished by flushing using both saline and higher viscosity liquids such as nonionic contrast and oxygenated perfluorodecalin [12]. Both future pig and rabbit studies are still planned to help identify possible weak points in all aspects of our system. Data acquisition was limited to a rate of 4 frames per second as to not break the electrical slip ring due to over-rotation of the probe. Figure 3 shows a side by side comparison of a slice from a human coronary sample with two areas of plaque shown, the first showing a plaque built up along the arterial wall and second showing a thin fibrous cap which IVUS is able to penetrate past further. 3D rendering is possible using a ray tracing algorithm using the OpenGL library with stacked frames serving as the texture map. Post processing 3D is done with commercial software which provides improved resolution and functionality. Figure 4 shows a stack of 1000 slices from the same sample with a translational resolution of 10 um. The authors wish to thank individuals who donate their bodies and tissues for the advancement of education and research.

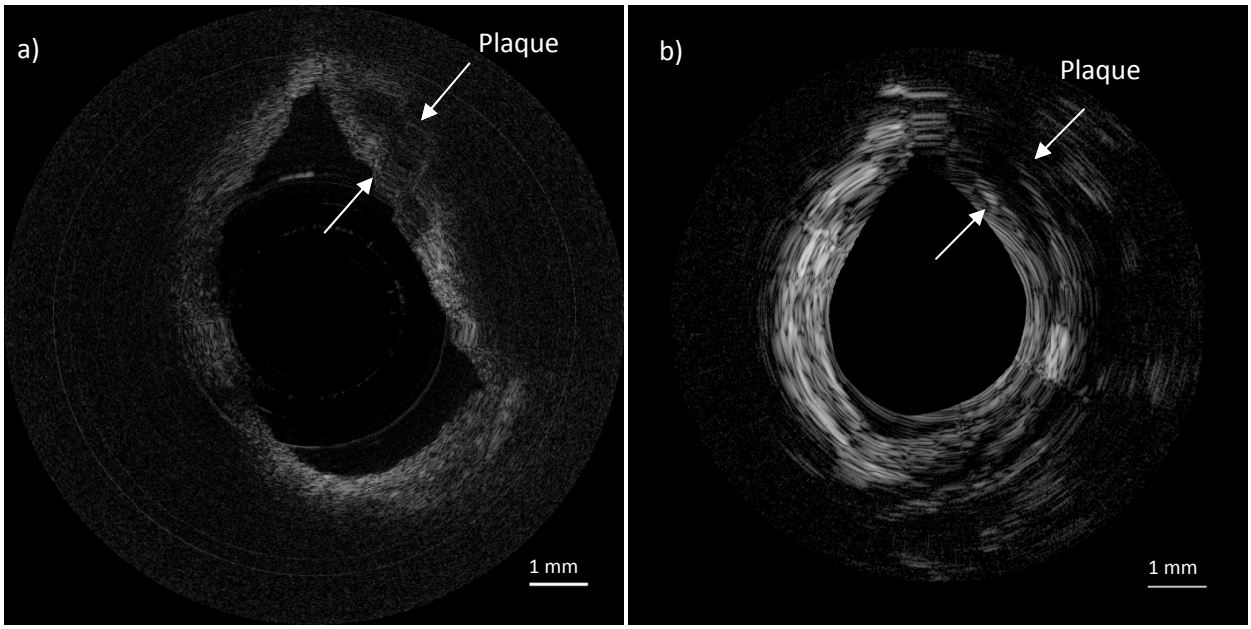

Fig. 5. (a) OCT and (b) IVUS slice of human coronary artery

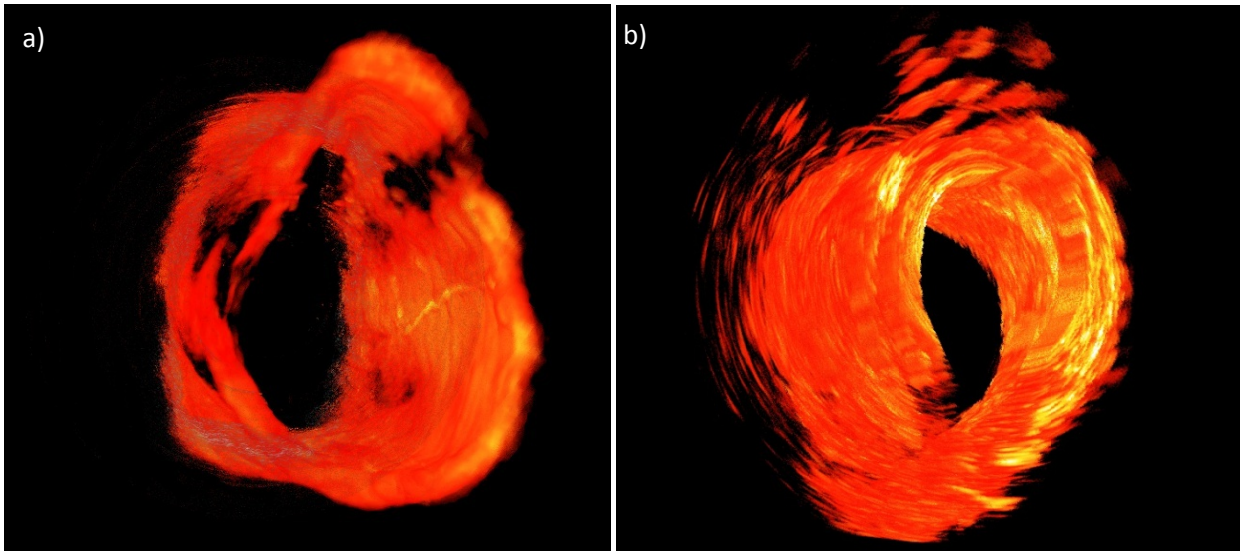

Fig. 6. 3D reconstruction of 1000 slices of (a) OCT and (b) IVUS images from human coronary artery

References

1. Roger VL, Go AS, Lloyd-Jones DM, et al., American Heart Association Circulation. 2011; 123(4):e18–e209
2. L.P. Hariri et al, Biomed. Opt. Express **1**, 566-573 (2010)
3. M. U. Farooq, A. Khasnis, A. Majid, and M. Y. Kassab, Vascular Medicine **14**(1), 63–71 (2009)
4. G. J. Tearney, I. K. Jang, and B. E. Bouma, J. Biomed. Opt. **11**(2), 021002 (2006)
5. T. Sawada et al., European Heart Journal **29**(9), 1136–1146 (2008)
6. X. Li, J.C. Yin, C.H. Hu, Q.F. Zhou, K.K. Shung, Z.P. Chen, Appl. Physics Letters, **97**(13), 133702 (2010)
7. J.C. Yin, H.C. Yang, X. Li, J. Zhang, Q.F. Zhou, C.H. Hu, K.K. Shung, Z.P. Chen, J. Biomed. Opt, **15**(1), 010512 (2010)
8. J. Yin et al., J. Biomed. Opt. **16**, 060505 (Jun 02, 2011)
9. Y. Yasuno et al., Opt. Express **13**, 10652-10664 (2005)

10. C. Sigg, M. Hadwiger, GPU Gems 2: Programming Techniques for High-Performance Graphics and General-Purpose Computation, 313–329 (2005)
11. D. Ruijters, B.M. Romeny, P. Suetens, In Proc. Tenth IASTED International Conference on Computer Graphics and Imaging, 117-122 (2008)
12. K. C. Hoang et al., J.Biomed. Opt. 14(3), 034028 (2009)